Carcinogenesis, 2020, Vol. 41, No. 10, 1409–1420

doi:10.1093/carcin/bgz205
Advance Access Publication January 7, 2020
Original Article

ORIGINAL ARTICLE

Epidermal *ROCK2* induces AKT1/GSK3β/β-catenin, NFκB and dermal tenascin C; but enhanced differentiation and p53/p21 inhibit papilloma

Siti F.Masre,[1,4] Nicola Rath[2], Michael F.Olson[3] and David A.Greenhalgh[1,*]

[1]Section of Dermatology and Molecular Carcinogenesis, School of Medicine, Dentistry and Nursing, College of Medical, Veterinary and Life Sciences, Glasgow University, Glasgow G31 2ER, UK, [2]Molecular and Cellular Biology Laboratory, Cancer Research UK, Beatson Institute for Cancer Research, Garscube Estate, Glasgow G61 1BD, UK and [3]Department of Chemistry and Biology, Ryerson University, Ryerson MaRS Research Facility MaRS Discovery District, West Tower 661 University Avenue Toronto, Ontario, Canada M5G 1M1 [4]Present address: Centre of Health and Applied Sciences, Faculty of Health Sciences, National University of Malaysia, 50300 Kuala Lumpur, Malaysia

*To whom correspondence should be addressed. Tel: +44 141 201 8603; Email: david.greenhalgh@glasgow.ac.uk

Abstract

ROCK2 roles in epidermal differentiation and carcinogenesis have been investigated in mice expressing an RU486-inducible, 4HT-activated ROCK2 transgene (*K14.creP/lslROCK*^{er}). RU486/4HT-mediated ROCK^{er} activation induced epidermal hyperplasia similar to cutaneous oncogenic *ras*^{Ha} (*HK1.ras*); however ROCK^{er} did not elicit papillomas. Instead, anomalous basal-layer ROCK^{er} expression corrupted normal ROCK2 roles underlying epidermal rigidity/stiffness and barrier maintanance, resulting in premature keratin K1, loricrin and filaggrin expression. Also, hyperproliferative/stress-associated keratin K6 was reduced; possibly reflecting altered ROCK2 roles in epidermal rigidity and keratinocyte flexibility/migration during wound healing. Consistent with increased proliferation, *K14.creP/lslROCK*^{er} hyperplasia displayed supra-basal-to-basal increases in activated p-AKT1, inactivated p-GSK3β^{ser9} and membranous/nuclear β-catenin expression together with weak NFκB, which were absent in equivalent *HK1.ras* hyperplasia. Furthermore, ROCK^{er}-mediated increases in epidermal rigidity via p-MypT1 inactivation/elevated MLC, coupled to anomalous β-catenin expression, induced tenascin C-positive dermal fibroblasts. Alongside an altered ECM, these latent tenascin C-positive dermal fibroblasts may become putative pre-cancer–associated fibroblasts (pre-CAFs) and establish a susceptibility that subsequently contributes to tumour progression. However, anomalous differentiation was also accompanied by an immediate increase in basal-layer p53/p21 expression; suggesting that while ROCK2/AKT1/β-catenin activation increased keratinocyte proliferation resulting in hyperplasia, compensatory p53/p21 and accelerated differentiation helped inhibit papillomatogenesis.

Introduction

ROCK2, a major effector of cytoskeletal architecture, regulates cellular flexibility/tension to maintain tissue rigidity and cellular motility in response to wounding or disease (1–4). This is achieved through regulation of actomyosin contraction via phosphorylation of myosin regulatory light chains (p-MLC) and the myosin-binding subunit of the MLC phosphatase (p-Mypt1) that subsequently interface with numerous signalling pathways (3,4). In skin, this mechano-signalling system is an essential component that contributes to keratinocyte proliferation and differentiation to maintain epidermal homeostasis and barrier function (5–7). ROCK family members are also required for epidermal formation (7) and together with appropriate intermediate filament (IF) expression (8), influence keratinocyte proliferation, and differentiation in terms of rigidity and flexibility. For instance, deregulation of ROCK2-mediated actomyosin-mediated cellular tension in cutaneous keratinocytes leads to

Received: September 23, 2019; **Revised:** December 21, 2019; **Accepted:** January 3, 2020

Abbreviations

CAF	cancer-associated fibroblast
ECM	extracellular matrix
IF	intermediate filament
p-MLC	phosphorylation of myosin regulatory light chain
p-Mypt1	myosin-binding subunit of the MLC phosphatase
pre-CAF	pre-cancer–associated fibroblast.

collagen deposition and increased skin rigidity (6). Increased matrix density subsequently changes integrin clustering, alters focal adhesions and establishes a mechano-transduction feedback loop that influences keratinocyte proliferation via FAK-mediated, α6/β4 integrin signalling (9,10). In turn, altered focal adhesion signalling through FAK/AKT activation downregulate GSK3β to increase β-catenin expression; with corresponding consequences for epidermal proliferation, differentiation and disease (1–4,6). In determination of keratinocyte motility/flexibility, ROCK1 and ROCK2 have separate roles in regulation of focal adhesion turnover (5,9) while in wounding, ROCK2 expression affects the migrating edge of full thickness wounds and overexpression accelerates healing (2).

In human carcinogenesis, failures in ROCK2 signalling resulting in increased actomyosin-mediated cellular tension and collagen deposition gives a rigid extracellular matrix (ECM) (3,6) that provides a matrix permissive for tumour progression (11,12). In response to increased tissue stiffness, additional anomalous Rho-ROCK/β-catenin signalling has paracrine effects on specific dermal cells that remodel novel collagen fibres or alter expression of specific ECM molecules (13–15). These modifications then provide the highways for invasion that are exploited by ROCK-modified cells possessing inherent changes to their actomyosin cytoskeleton resulting in the mechano-transduction abilities necessary to change cell shape and alter motility (1,3,6,12–15). Thus, given the lack of successful anti-ras therapies, in being downstream of ras signalling (3,4), the Rho kinase family have become attractive targets for potential therapy (16,17).

In transgenic mice, epidermal expression of inducible ROCK2 [*K14.ROCK*^{er}] enhanced malignant conversion following two-stage DMBA/TPA chemical carcinogenesis manifest by increased tissue rigidity (6). Similarly, *ROCK*^{er} activation co-operated with epidermal ras^{Ha} activation [*HK1.ras*] to induce malignant conversion via p53 loss, increased p-Mypt1 and tenascin C overexpression, which altered the ECM to facilitate invasion (18). *HK1.ras/K14.ROCK*^{er} mice also identified ROCK^{er}-associated synergism with NF-κB and AKT1 overexpression in late-stage papillomatogenesis that aided conversion to malignancy; together with p21-associated inhibition of early malignant progression (18). Indeed, malignancy depended on continued ROCK^{er}/p-AKT1/NF-κB activation, as 4HT-cessation caused tumour regression via intense p21 [not p53] expression that identified an antagonism between *p21* and endogenous ROCK2, which also targeted AKT1/NF-κB activation (18–20). Nonetheless, despite ROCK2 being an effector of ras^{Ha} signalling, and a potent regulator of AKT/GSK3β/β-catenin/FAK axis etc, ROCK^{er} expression alone failed to exhibit papillomas (6,18).

Therefore, to investigate potential mechanism(s) that inhibited ROCK^{er}-mediated papillomatogenesis, ROCK2, p53, p21, AKT/GSK3β/β-catenin and NF-κB status were assessed, together with tenascin C, and results contrasted to hyperplasia produced in *HK1.ras* mice; a model that produces wound-dependent papillomas with 100% penetrance (21). Three themes responded to mechanical stress induced by ROCK^{er} expression in *K14.creP/lslROCK*^{er} hyperplasia. Two underlie inhibition of papillomatogenesis involving changes in differentiation marker expression [keratins K1, K6α, loricrin, filaggrin] that highlight a premature/accelerated commitment to differentiation and alter keratinocyte flexibility/motility; and responses to deregulated AKT/GSK3β/β-catenin axis that induce compensatory p53/p21 expression to inhibit papillomatogenesis. The third found appearance of dermal, tenascin C-positive fibroblasts that maybe precursors of subsequent cancer-associated fibroblast populations [pre-CAFs] (13,14); suggesting ROCK^{er}-altered dermal ECM established at an early stage may persist to provide a latent oncogenic susceptibility that subsequently contributes to malignant conversion.

Materials and methods

Transgenic genotypes and induction of phenotypes

CAGG-lsl-ROCK^{ER} mice express a 4HT-inducible ROCK2/oestrogen receptor fusion transgene such that following Cre activity, ROCK^{er} is expressed from a ubiquitous *CAGG* promoter (22). To achieve epidermal-specific ROCK^{er} expression, *CAGG-lsl-ROCK*^{er} were crossed to mice expressing a keratin K14-driven Cre fusion protein [*K14.creP* (23,24)], where following topical treatment with RU486, bi-genic *K14.creP/lslROCK*^{er} cohorts expressed ROCK^{er} protein in all epidermal layers and hair follicles. Mice expressing epidermal activated ras^{Ha} from a modified keratin-K1 promoter [*HK1.ras*] have been reported previously (21). Genotypes were identified by PCR employing primers:

lslROCK^{er}: 1 fwd: 5′-CGACCACTACCAGCAGAACA-3′; 2 rev: 5′-GAC GAACCAACTGCACTTCA-3′

K14creP: fwd: 5′-TCATTTGGAACGCCCACT-3′; rev: 5′-GATCCGAAT AACTACCTGTTTTG-3′

HK1.ras: fwd: 5′-GGATCCGATGACAGAATACAAGC-3′; rev: 5′-ATC GATCAGGACAGCACACTTGCA-3′

Epidermal-specific ROCK^{er} expression was achieved by topical treatment of *K14.creP/lslROCK*^{er} skin with 2.5 μg RU486/3 × 15 μl ethanol/week for 3 weeks (mefipristone, Sigma, Gillingham, UK), with controls receiving ethanol alone. ROCK^{er} activation via the modified oestrogen receptor HBD (mERTM), which binds the non-physiological ligand, 4-hydroxytamoxifen (4HT;Sigma), was achieved by thrice weekly treatments of 330 μg 4HT/15 μl ethanol delivered to the dorsal ear skin and back (1 mg/mouse). Control mice received vehicle alone. Each cohort comprised 10 male and three vehicle controls in repeat experiments, maintained for 12, 20 and 30 weeks to assess papillomatogenesis. The ROCK:ER fusion protein, in which the ROCK2 kinase domain has been inserted between GFP and the hormone-binding domain of a mutated oestrogen receptor (ER) has been used previously to conditionally activate ROCK signalling (25) (Figure 1). In the absence of an oestrogen-like ligand such as tamoxifen, kinase activity is undetectable, while ligand stimulation results in the phosphorylation of genuine ROCK substrates including regulatory myosin light chains (MLC), the myosin-binding subunit of the myosin phosphatase complex (MYPT1) and the LIM kinases LIMK1 and LIMK2. The absence of activity without ligand stimulation and conditional activation by tamoxifen allows for precise control of the timing, duration and localization of ROCK activation in cells and tissues (25). One caveat that should be acknowledged is that, although the ROCK:ER fusion protein has been validated against previously characterized ROCK substrates, the possibility exists that additional substrates might also be phosphorylated. All experiments adhered to UK regulations; PPL60/4318 licenced to DAG.

Histology, immunofluorescence/ immunohistochemistry and western analysis

Skin biopsies were fixed in buffered formalin (24 h at 4°C) for haematoxylin and eosin staining or snap-frozen in liquid nitrogen and stored (–70°C). For differentiation analysis via double-label immunofluorescence, following antigen retrieval (5 min boil/10 mM sodium citrate), paraffin sections were

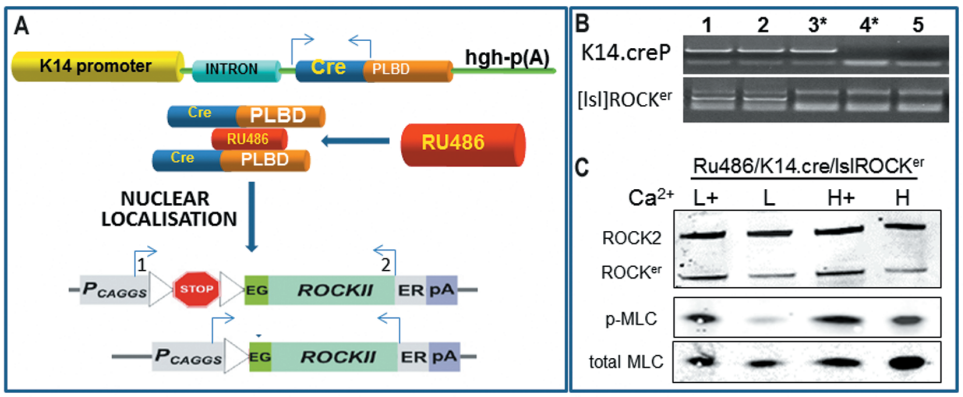

Figure 1. Schematic of K14.creP/lslROCK^{er} system and conformation of ROCK^{er} activation. (**A**) K14 promoter drives expression of a Cre recombinase–progesterone ligand binding domain (PLB) fusion protein (*K14.creP*) and following RU486 treatment, CREP ablates a *loxP*-flanked stop cassette to express ROCK^{er} from the CAGG promoter (*CAGGS-lslROCK^{er}*). (**B**) PCR analysis of RU486-treated *K14.creP/lslROCK^{er}* skin identifies *K14.creP* (~600 bp; lanes 1–3); primers 1/2 (arrows) identify the ablated stop codon band at ~500 bp and full-length product (~575bp) in untreated epidermis and non-epidermal tissue (lanes 1 and 2), untreated (lane 3*) or *CAGGS-lslROCK2^{er}* alone DNA (ethanol/lane 4*; RU486/lane 5). (**C**) *Conformation of ROCK^{er} activation*. Primary *K14creP.lslROCK^{er}* keratinocytes cultured in RU486 under proliferative low (L: 0.05 mM) or differentiating (H: 0.12 mM) calcium concentrations, with or without 1 nM 4HT (L+; H+) show ROCK^{er} increases following 4HT-treatment. ROCK2 activity determined by phospho-MLC expression, increases on induction of differentiation and increases further following additional 4HT-mediated ROCK^{er} activation. Total MLC served as a loading control.

incubated overnight (4°C) with: rabbit anti-K1, anti-K6, anti-loricrin, anti-filaggrin [diluted 1:100 (Covance, Richmond, CA)] employing guinea-pig anti-K14 antibodies [1:400 (Fitzgerald, Acton, MA)] to delineate epidermis; and visualized by biotinylated-goat anti-guinea pig/Streptavidin-Texas Red [1:100/1:400 (Vector Labs)] or fluorescein isothiocyanate-labelled anti-rabbit IgG [diluted 1:100 (Jackson Labs, West Grove, PA)]. Sections were analysed by immunofluorescence for expression of: p-AKT1 [1:100 (Abcam #81283 Cambridge, UK; Santa Cruz p-AKT1/2/3 sc-7985-R)]; β-catenin [1:50 (Abcam; 1:100 sc#1496-R)]. For BrdU labelling, mice were injected IP with 125 mg/kg 5-bromo-4-deoxyuridine (Sigma) 2 h before biopsy. Following antigen retrieval, BrdU-labelled cells were identified by overnight incubation (4°C) with fluorescein isothiocyanate-conjugated anti-BrdU [1:5 (Becton Dickinson)]. The numbers of positive cells were counted in three images of separate stained sections from five different mice per cohort and mitotic index expressed as BrdU-labelled cells per mm of basement membrane.

For immunohistochemical analysis, following antigen retrieval, paraffin sections were incubated overnight (4°C) with: rabbit anti-p53 1:50; sc#6243 Santa Cruz, Autogen Bioclear, Wiltshire, UK) and confirmed by Abcam (#131442 at 1/50); anti-p21^{WAF} (1:50; sc#397; confirmed by Proteintech #10355-1-AP (1:250); anti-ROCK2 (1:100; sc#5561), β-catenin (1:150; sc#1496-R), confirmed by Abcam (1/50; #32572); anti-p-GSK3β (1:50; sc#11757); rabbit anti-phospho-Mypt1^{Thr696} (1:50; Millipore AbS45, Watford, UK); rabbit anti-tenascin C (1:50; Sigma #T2551); rabbit anti-NF-κB p65 (1:600; Abcam #16502); total GSK3β (1:200, Abcam #32391); and rabbit anti-GFP (1:50; Clonetech, Takara Bio Europe, Saint-Germain-en-Laye, France) followed by HRP-conjugated goat anti-rabbit (1:100; Vector) and visualized by DAB+ staining (Dako, Amersham Biosciences, Little Chalfont, UK). Photomicrographs employed Axiovision image capture software (Zeiss Microscopes, Cambridge, UK). Quantitative analysis of the images (averaged from six separate areas) was performed using ImageJ software (ImageJ version 1.46r; National Institute of Health, Bethesda) and statistical analysis employed one-way analysis of variance (ANOVA) with post hoc testing using SPSS software (version 22.0, IBM Corporation). For quantitation of dermal tenascin C^{+ve} cells, counts were averaged from 10 micrographs, taken from analysis of three separate animals per 12 weeks cohort, and compared with untreated or RU486-alone controls and RU486/4HT-treated *HK1.ras* mice. Results are expressed as numbers of positive cells per 0.25 mm skin and ANOVA statistical analysis.

For western analysis, primary keratinocytes were isolated from newborn epidermis and seeded at 5 × 10^6/60 mm dish and cultured in fibroblast conditioned, Dulbecco's modified Eagle's medium/10% chelated fetal calf serum/0.05 mM Ca^{2+} (26) for 4 days, with/without 5 × 10^{-9} M RU486; or 4HT (1 nM; Sigma); then maintained in low (0.05 mM) calcium or high (0.12 mM) calcium media with/without 4HT (1 nM) for 3 days. Cell lysates were prepared in lysis buffer (1% SDS/50 mM Tris pH 7.5) containing Protease inhibitor P-8340 (1:100; Sigma) and for keratin westerns, following centrifugation, pellets were re-suspended in keratin extraction buffer (10 mM Na-phosphate pH 8.0/2 mM $MgCl_2$/1 mM EDTA/2 mM DTT) homogenized and centrifuged (13 000*g* rpm/10 min). Supernatants were added to 200 µl 2× SDS gel-loading buffer (100 mM Tris pH 6.8/4% SDS/10% glycerol/200 mM DTT/0.1% bromophenol blue) homogenized and stored at –20°C. Protein concentration was determined by bicinchoninic assay (Sigma) and proteins separated by 10% SDS-PAGE electrophoresis and western blot analysis performed employing antibodies to: rabbit anti-K1, anti-K6 (1:1000 in 12% bovine serum albumin-phosphate-buffered saline); anti-ROCK1/2 (Millipore 07-1458), anti-p-MLC2 (p-Ser^{19}), and anti-tMLC (1:500; Cell Signalling Technology) and expression detected by Alexa-Fluor 680 (Thermo-Fisher Scientific) secondary antibody and infrared imaging (Li-Cor Odyssey). Quantitative image analysis employed ImageJ software (ImageJ version 1.46r; National Institute of Health, Bethesda) and statistical analysis employed one-way ANOVA (version 22.0, IBM Corporation).

Results

ROCK^{er} activation induces epidermal hyperplasia without papillomatogenesis

RU486/4HT-treated *K14.creP/lslROCK^{er}* mice, expressing 4HT-activated ROCK^{er} from a Cre-responsive CAGG promoter, displayed epidermal hyperplasia but lacked papillomas. ROCK^{er} expression in *K14.creP/lslROCK^{er}* epidermis and cultured keratinocytes was confirmed PCR and western analysis (Figure 1A–C); while phosphorylation of myosin light chain protein (p-MLC) confirmed 4HT-mediated ROCK^{er} activation in proliferative (low Ca^{2+}) and differentiating (high Ca^{2+}) conditions (Figure 1C). *In vivo*, despite thrice-weekly 4HT treatments more than 12, 20 or 30 weeks (n = 10/cohort), no overt papillomas appeared (Figure 2A) and RU486/4HT-treated *K14.creP/lslROCK^{er}* mice exhibited ear thickening with mild keratosis by weeks 8–10; which regressed if 4HT was withheld. Histological analysis of RU486/4HT-treated *K14.creP/lslROCK^{er}* mice revealed mild epidermal hyperplasia compared with normal RU486-treated control skin (Figure 2B–D), consistent with GFP-tag expression (Figure 2E and F), that confirmed ROCK^{er} expression, being absent in untreated controls (Figure 2G). ROCK2 protein analysis revealed elevated ROCK2/ROCK^{er} expression in hyperplastic

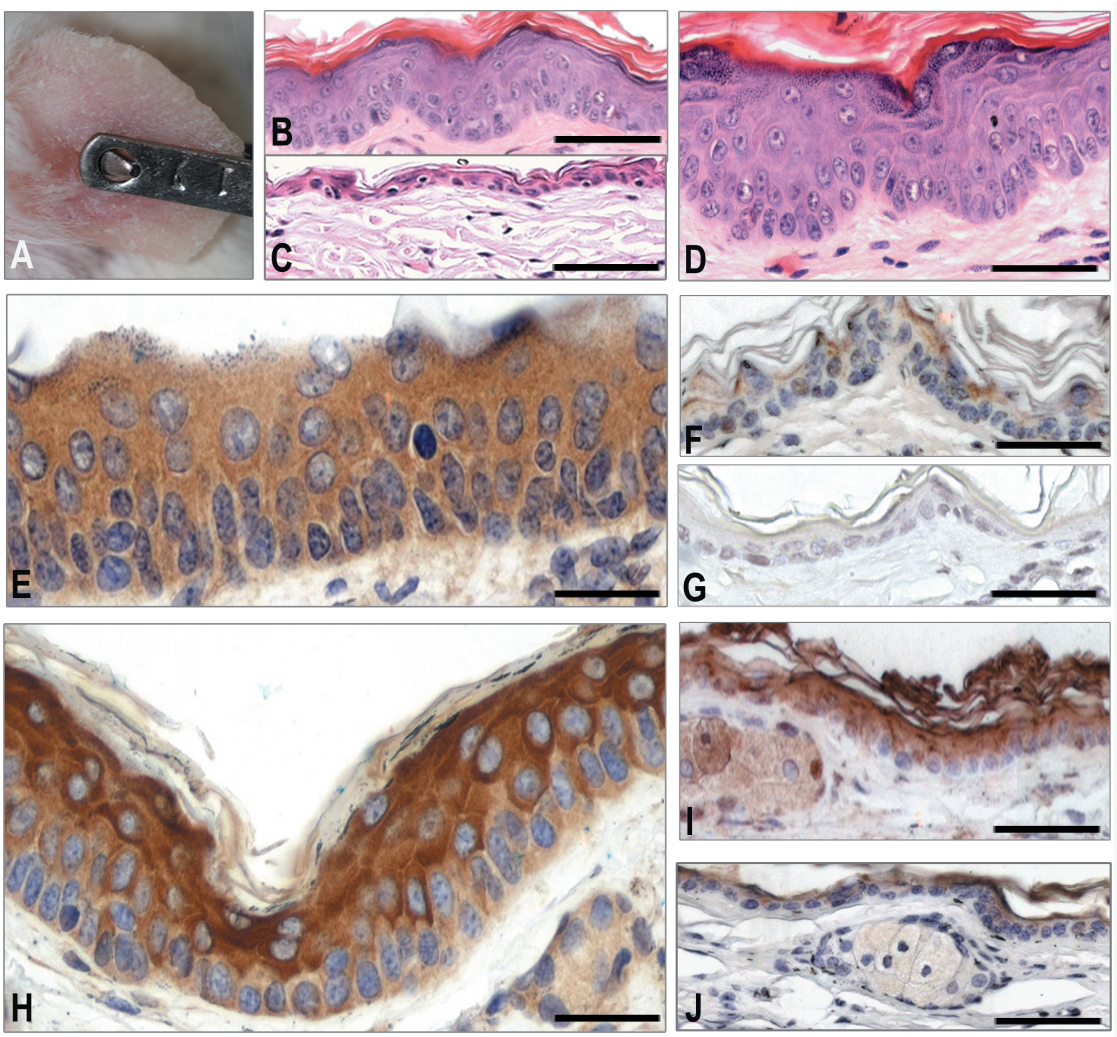

Figure 2. Conformation of ROCK^{er} expression in *K14.creP/lslROCK^{er}* phenotypes. (**A**) 4HT/RU486-treated *K14.creP/lslROCK^{er}* mice (20 weeks) exhibit mild keratosis but despite thrice-weekly treatments (up to 6 months), no papillomas appear. (**B**) 4HT/RU486-treated *K14.creP/lslROCK^{er}* mice exhibit mild epidermal hyperplasia (12 weeks) compared with (**C**) normal RU486-alone control skin (20 weeks) that (**D**) increases over time (20 weeks) but remains hyperplastic. (**E–G**) GFP-tag analysis of *K14.creP/lslROCK^{er}* skin confirmed ROCK^{er} expression in (E) hyperplastic 4HT/RU486-treated and (F) normal RU486-alone skin, was absent in (G) untreated controls. (**H–J**) Analysis of ROCK2/ROCK^{er} protein levels shows (H) hyperplastic *K14.creP/lslROCK^{er}* epidermis exhibits elevated expression following 4HT/RU486 alongside (I) RU486-alone controls; compared with lower, suprabasal expression in (J) normal epidermis. Bars: B ~80 μm; C–J ~40 μm; E and H ~30 μm.

RU486/4HT-treated *K14.creP/lslROCK^{er}* and normal RU486-treated *K14.creP/lslROCK^{er}* (Figure 2H and I); while endogenous ROCK2 expression in wild-type controls appeared mainly supra-basal (Figure 2J) consistent with roles in epidermal rigidity and barrier maintenance.

Differentiation marker expression implies inhibitory accelerated/premature differentiation

Given ROCK is an effector of ras signalling (3), yet failed to elicit papillomas, effects of ROCK^{er} expression on keratinocyte differentiation were investigated (Figure 3) and results contrasted to hyperplasia induced by ras^{Ha} activation (21). *In vitro*, western analysis showed activated ROCK^{er} elicited anomalous expression of differentiation marker keratin K1 in proliferating keratinocytes cultured in low calcium (Figure 3L left panel: L versus L+). Furthermore, hyperproliferative, wound associated keratin K6α, normally highly expressed in low calcium keratinocytes, was abnormally low in RU486/4HT-treated bi-genic *K14.creP/lslROCK^{er}* keratinocytes (Figure 3, L versus L+) returning to normality in differentiated high Ca^{2+} media (Figure 3, H versus H+). Quantitation of expression levels (Supplementary Figure S1, available at *Carcinogenesis* Online) confirmed significant increases in K1 expression (L+; $^{*}P < 0.01$) in *K14.cre/lslROCK^{er}* versus *lslROCK^{er}* keratinocytes cultured in proliferative low calcium conditions, compared with normal cells suggesting an altered, early differentiation; in addition the novel, unique decrease in K6α expression (L+; $^{**}P < 0.01$) also suggests either an early differentiation response or may reflect ROCK2 roles on K6α in these culture conditions that mimic mechanisms associated with wounding.

In vivo, immune fluorescence analysis of K1 and K6α expression (Figure 3A–D left panel: K1 ; Figure 3E–H left panel: K6] were investigated alongside late-stage differentiation markers filaggrin and loricrin (Figure 3A–D right panel: filaggrin; Figure 3E–H right panel: loricrin) employing keratin K14 to delineate the epidermis. RU486/4HT-treated *K14.creP/lslROCK^{er}* hyperplasia shows keratin K1 expression was mainly suprabasal (Figure 3A and B left panel), however the normally smooth

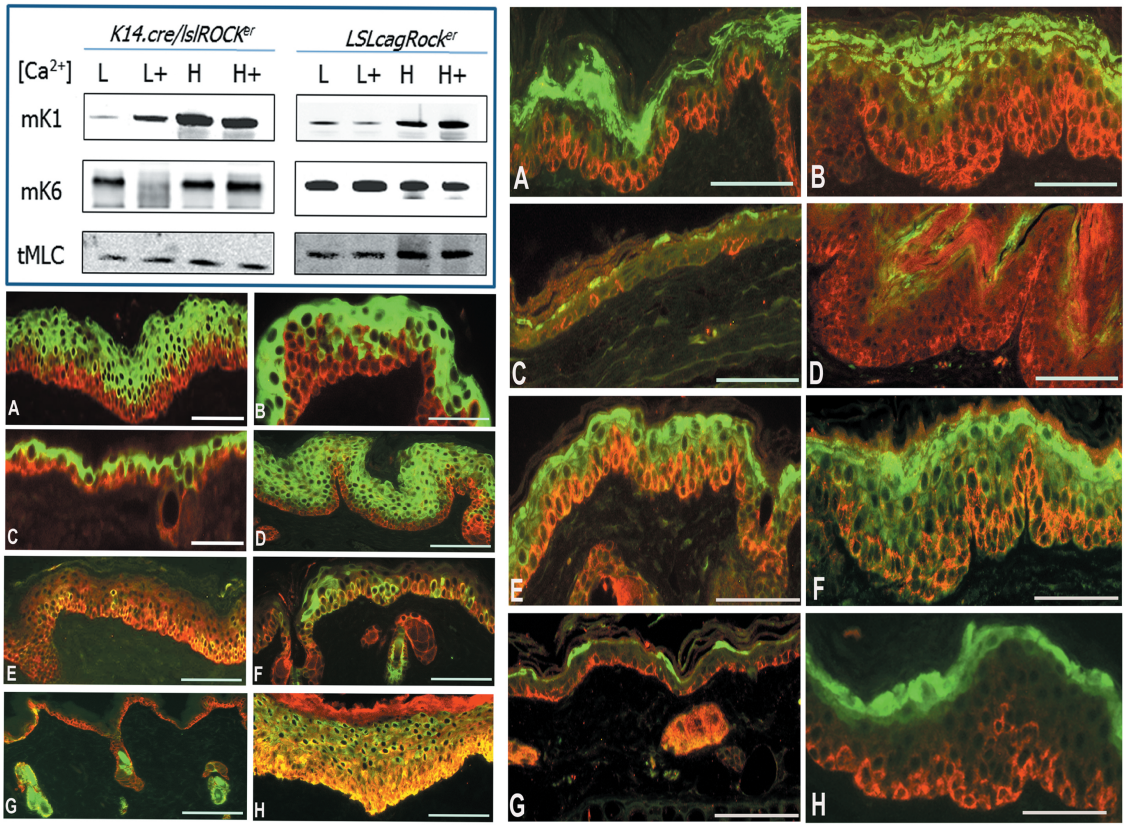

Figure 3. Analysis of differentiation marker expression. Western analysis of keratin K1/K6α expression: primary *K14creP.lslROCK*^{er} or control *lslcagROCK*^{er} keratinocytes are cultured in low or high calcium media (L = 0.05 mM; H = 0.12 mM) containing RU486 (5 nM) with/without 4HT (1 nM; L+/H+). ROCK^{er} activation induces anomalous K1 expression in low calcium medium, which was absent in untreated or 4HT-treated *lslROCK*^{er} controls (L+ versus L); with elevated K1 expression in high calcium similar to normal 4HT-treated *lslROCK*^{er} controls keratinocytes. ROCK^{er} activation also down-regulates K6α in hyperproliferative, low calcium *K14creP.lslROCK*^{er} keratinocytes (L+) compared with normal4HT–treated *lslROCK*^{er} controls. Total MLC served as a loading control. Expression level quantitation is given in Supplementary Figure S1, available at *Carcinogenesis* Online. Left: Immune fluorescence analysis of keratin K1 (**A–D**) and K6α (**E–H**) expression (green), counterstained for K14 (red) to delineate epidermis/dermis. (A and B) 4HT/RU486-treated *K14.cre/lsl.ROCK*^{er} hyperplasia display a ragged/disordered, supra-basal K1 profile, as proliferative K14^{+ve}-basal layer cells differentiate and transit into supra-basal keratinocytes. (C) None 4HT/RU486-treated control *K14.cre/lsl.ROCK*^{er} epidermis displays normal, supra-basal K1; while (D) *HK1.ras* hyperplasia exhibits an ordered K1 pattern at the K1/K14 transition border. (E) 4HT/RU486-treated *K14.cre/lsl.ROCK*^{er} and (F) *K14.ROCK*^{er} hyperplasia display patchy K6α expression compared with (G) normal epidermis with K6α restricted to hair follicles. (H) *HK1.ras* hyperplasia exhibits strong, uniform K6α. Bars: E, G and H, ~120 μm; A, D and F: ~70–80 μm; B and C: ~40 μm). Right panel: Filaggrin (**A–D**) and loricrin (**E–H**) expression in 4HT/RU486-treated *K14.cre/lsl.ROCK*^{er}. (A and B) Elevated filaggrin expression increases with increasing hyperplasia (12 and 30 weeks); showing (B) premature filaggrin detectable below the granular layer compared with (C) granular layer filaggrin in normal epidermis. (D) *HK1.ras* displays reduced filaggrin as hyperplasia increases. (E and F) Loricrin expression in treated *K14.cre/lsl.ROCK*^{er} hyperplasia (at 12 and 30 weeks) shows increased, premature expression becomes detectable in supra-basal layers. (G) Untreated *K14.cre/lsl.ROCK*^{er} epidermis exhibits granular loricrin expression; while (H) *HK1.ras* hyperplasia expresses reduced, granular loricrin. Bars: ~70–80 μm.

transition from proliferative basal to post-mitotic, supra-basal keratinocyte was not ordered; with numerous K1^{+ve} cells appearing in the expanded (K14^{+ve}) basal layers. This ragged transition from proliferative to differentiating keratinocytes contrasted with the ordered differentiation observed in either normal, RU486-treated *K14.cre/lslROCK*^{er} controls or *HK1.ras*-activated hyperplasia (Figure 3C and D left panel). Of note, normally keratin K6α expression is restricted to hair follicles becoming strongly expressed under stressed or hyperproliferative (wound) conditions; however RU486/4HT-treated *K14.creP/lslROCK*^{er} hyperplasia displayed reduced, patchy K6α expression (Figure 3E and F left panel) often localized to troughs of papillomatous (folded/convoluted) hyperplasia, which possibly reflect the altered epidermal rigidity/flexibility. In contrast, normal RU486-treated *K14.cre/lslROCK*^{er} epidermis exhibited K6α in hair follicles; while RU486/4HT-treated *HK1.ras* hyperplasia expressed strong, uniform K6α (Figure 3G and H left panel).

Further consistent with anomalous modification of ROCK2 roles in differentiation, 4HT-treated/RU486-*K14.cre/lslROCK*^{er} epidermis displayed elevated/premature expression of late-stage markers loricrin and filaggrin. ROCK^{er} activation resulted in persistent, elevated filaggrin expression; with premature staining appearing in supra-basal layers of increasing hyperplasia compared with controls (Figure 3A and D versus Figure 3C right panel). However, as *HK1.ras* hyperplasia increased, filaggrin expression reduced (Figure 3D right panel). Similarly, ROCK^{er} activation increased premature, supra-basal loricrin expression (Figure 3E and F: right panel); whereas *HK1.ras* hyperplasia exhibited loricrin expression confined to granular layers similar to normal (Figure 3G and H: right panel). This elevated, premature filaggrin/loricrin expression would thus contribute to the increased epidermal rigidity observed in ROCK^{er} mice and strengthen roles for ROCK2 in maintaining barrier function.

ROCK^{er} hyperplasia displays elevated basal-layer β-catenin, GSK3β inactivation and AKT1 activation

Previous analysis of ROCK-activated epidermis revealed increased β-catenin expression associated with AKT-mediated

GSK3β inactivation (6) thus given the lack of ROCK^{er}-mediated papillomatogenesis and increased differentiation responses, the β-catenin/GSK3β/AKT signalling axis was investigated and again cell/tissue localization contrasted to *HK1.ras*-induced hyperplasia. Analysis of β-catenin expression in 4HT/RU486-treated *K14.creP/lslROCK^{er}* epidermis demonstrated increased expression in areas of 4HT-treated versus untreated skin (Figure 4A–C). Over time, increasing ROCK^{er}-mediated hyperplasia displayed elevated, membranous β-catenin expression in both basal and supra-basal epidermis (Figure 4C) with detectable cytoplasmic/nuclear expression in basal layer keratinocytes (Figure 4D). In contrast, 4HT/RU486-treated *HK1.ras* retained a mainly membranous β-catenin profile in supra-basal keratinocytes (Figure 4E). Quantitation (via image J analysis) of treated versus untreated areas (Figure 4A and B) show a significant difference in expression levels ($^{\#}P < 0.0001$; Supplementary Figure S2, available at *Carcinogenesis* Online); a result repeated in equivalent immunohistochemical analysis (Supplementary Figure S3, available at *Carcinogenesis* Online). In comparison with *HK1.ras* hyperplasia, β-catenin expression in 4HT/RU486-treated *K14.creP/lslROCK^{er}* epidermis was again significantly increased ($^{**}P < 0.0001$); with supra-basal β-catenin expression in *HK1.ras* remaining similar to supra-basal, membranous β-catenin levels of normal epidermis.

Similarly, early 4HT/RU486-treated *K14.creP/lslROCK^{er}* epidermis (4 weeks) shows elevated p-GSK3β expression in 4*HT*-treated versus untreated ear skin (Figure 4F) which was maintained in older hyperplastic skin (12 weeks; Figure 4G) where elevated p-GSK3β parallels β-catenin expression in both proliferative basal and differentiated supra-basal layers (Figure 4H versus Figure 4D). 4HT/RU486-treated *HK1.ras* hyperplasia (4 weeks) displays a less intense, diffuse p-GSK3β profile that with time and increasing papillomatous hyperplasia (8–10 weeks) showed reduced basal layer and increasingly supra-basal p-GSK3β expression; which again parallels β-catenin expression in *HK1.ras* hyperplasia (Figure 4I versus Figure 4E). Image quantitation (Supplementary Figure S4, available at *Carcinogenesis* Online) of 4HT/RU486-treated *K14.creP/lslROCK^{er}* ears demonstrated elevated p-GSK3β expression in the upper treated dorsal skin versus lower untreated inner skin (Figure 4F) ($^{\#}P < 0.05$ RU/tam ROCK versus no tam ROCK) and was maintained over time compared with levels in *HK1.ras* epidermis at 4 weeks ($^{*}P < 0.001$) and 8 weeks ($^{**}P < 0.001$).

Analysis of p-AKT1 shows that *ROCK^{er}*-activation increased expression in 4HT/RU486-treated basal layers compared with normal RU486-treated *K14.creP/lslROCK^{er}* which possessed only sporadic, supra-basal p-AKT1^{+ve} keratinocytes (Figure 4J and K versus Figure 4L). Normal, neonatal epidermis (~24 h) with a naturally hyperplastic epidermis also exhibited elevated p-AKT1, but expression was restricted to supra-basal layers (Figure 4M). Older (12 weeks) 4HT/RU486-treated *K14.creP/lslROCK^{er}* epidermis retained elevated interfollicular p-AKT1, which paralleled β-catenin/p-GSK3β expression, suggesting ROCK^{er} established a return to a more juvenile epidermal context, possibly as a consequence of β-catenin expression (27); although here p-AKT1 exhibited supra-basal expression also (Figure 4N); possibly due to compensatory p53/p21 expression (see below), which helped inhibit papillomatogenesis. In contrast, 4HT/RU486-treated *HK1.ras* hyperplasia expressed lower, supra-basal p-AKT1 (Figure 4O) that with time reduced further to give a sporadic, supra-basal p-AKT1 expression similar to normal interfollicular epidermis (Figure 4L); suggesting AKT1 activation becomes causal later in ras-driven carcinogenesis. Image quantitation (Supplementary Figure S5, available at *Carcinogenesis* Online) shows 4HT/RU486-treated *K14.creP/lslROCK^{er}* skins expressed significant increases in p-AKT1 levels compared with untreated areas ($P < 0.0001$); including comparison with increased, suprabasal p-AKT1 expression exhibited by neonatal epidermis ($P < 0.001$). Over time elevated supra-basal p-AKT1 expression was maintained in 4HT/RU486-treated *K14.creP/lslROCK^{er}* epidermis compared with the low, sporadic levels observed in equivalent *HK1.ras* hyperplasia ($P < 0.0001$).

Elevated p-Mypt1 suggests changes in actomyosin-mediated contractility while cell-specific tenascin C highlights alterations in dermal ECM

Previously ROCK^{er} activity altered ROCK2 signalling and increased phosphorylation of myosin-binding subunit of MLC phosphatase complex 1 (Mypt1) to inactivate MLC-phosphatase activity; increase actomyosin-mediated cellular tension; collagen deposition in the dermal ECM and overall skin rigidity (6). Thus to both confirm ROCK^{er} activity and indirectly the resultant epidermal rigidity, p-Mypt1 levels were investigated (Figure 5) alongside tenascin C expression, an important ECM protein associated with tumour progression and ROCK signalling (15,28) that also reflects changes in ECM. In 4HT-treated *K14.creP/lslROCK^{er}* hyperplasia, ROCK^{er} expression increased expression of phosphorylated Mypt1 (p-Mypt1; Figure 5A and B), consistent with increased tissue rigidity (6); whereas control, RU486-treated *K14.creP/lslROCK^{er}* epidermis exhibited little detectable p-Mypt1 (Figure 5D; $^{*}P < 0.001$ A and B versus D). *HK1.ras* hyperplasia also expressed low p-Mypt1 levels, confined to supra-basal layers (Figure 5C; $^{**}P < 0.001$ A and B versus C), and given this weak p-Mypt1 yet uniform K6α (Figure 3), support the idea that ROCK^{er}/p-Mypt1-mediated changes in keratinocyte motility/contractility via altered actinomyosin-mediated mechanotransduction contributed to the reduced, sporadic K6α profile.

Tenascin C analysis (Figure 5F–I) investigated whether early, pre-neoplastic stages exhibited changes in ECM (15,28) that predispose to neoplasia, becoming causal later in malignant conversion/progression/tissue invasion; as observed in ROCK^{er}/ras^{Ha} carcinogenesis (18). RU486-4HT-treated *K14.creP/lslROCK^{er}* hyperplasia (Figure 5F) shows little epidermal tenascin C but dermis exhibited numerous tenascin C^{+ve} cells, absent in normal or RU486-treated *K14.creP/lslROCK^{er}* dermis (Figure 5G) and fewer in *HK1.ras* hyperplasia (Figure 5H). *ROCK^{er}*-associated dermal tenascin C^{+ve} cells also exhibited a diffuse peri-cellular halo suggesting expression in the local ECM; whereas in *HK1.ras* dermis, tenascin C^{+ve} cells exhibited a sharp, membranous expression (Figure 5F–H). Quantitation of dermal tenascin C^{+ve} cell numbers (Figure 5I) demonstrated *K14.creP/lslROCK^{er}* possessed approximately 3-fold increase in tenascin C^{+ve} cell numbers (19.43 ± 2.21) (as did 4HT treated *K14.ROCK^{er}* (18.40 ± 1.43) (6,18); compared with *HK1.ras*-induced hyperplasia (7.09 ± 1.43; $P < 0.05$); with a five-fold increase ($P < 0.01$) over normal, RU486-treated *K14.creP/lslROCK^{er}* (3.6 ± 0.55) or RU486-4HT-treated wild-type skin (3.45 ± 0.47). This tenascin C expression may link ROCK^{er}/β-catenin-associated increased collagen deposition (6) to effects of anomalous epidermal β-catenin expression on specific dermal fibroblast populations (14); and also suggests that once laid down by tenascin C^{+ve} cells, resultant ECM-associated changes coupled to tissue rigidity persists to aid/predispose to subsequent tumour progression (12).

ROCK^{er} hyperplasia displays increased p53/p21 expression responses that inhibit papillomatogenesis and limit NF-κB expression

Given these potent data on the AKT/GSK3β/β-catenin axis and the changes in ECM, the lack of papillomatogenesis compared

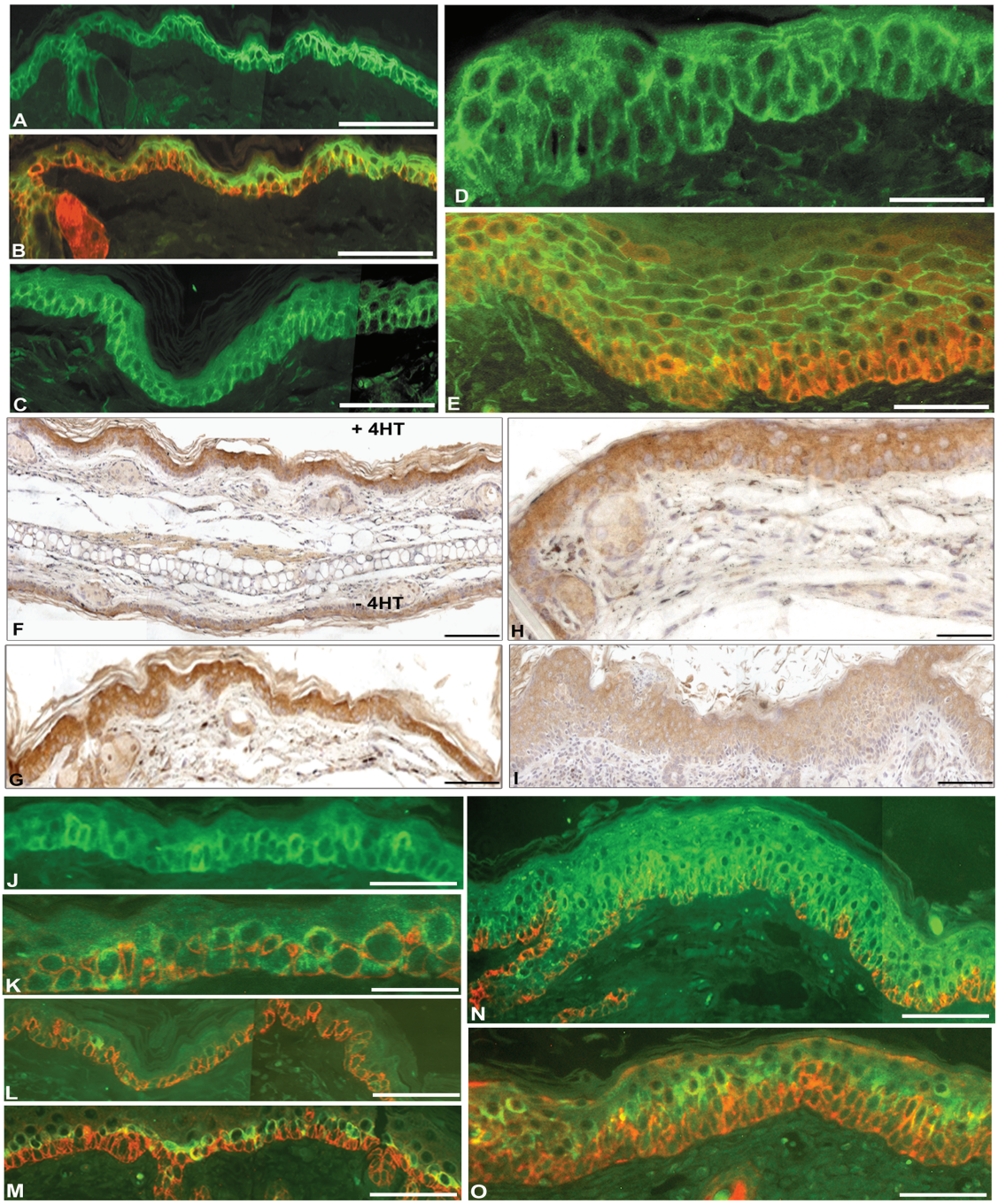

Figure 4. Analysis of β-catenin, p-GSK3β and p-AKT1 expression. (**A** and **B**) β-catenin expression in *K14.creP/lslROCK*^{er} epidermis (4–6 weeks) at the junction between RU486 alone (left) and 4HT/RU486-treatment (right) shows expression increases in 4HT-treated areas [B: double-label versus K14 (red) counterstain]. (**C**) Older 4HT/RU486-treated *K14.creP/lslROCK*^{er} hyperplasia (10 weeks) shows elevated β-catenin in basal and supra-basal layer keratinocytes. (**D**) Higher magnification of *K14.creP/lslROCK*^{er} epidermis (10 weeks) shows detectable cytoplasmic/nuclear β-catenin expression in basal layer keratinocytes compared with (**E**) *HK1.ras* hyperplasia (8 weeks) which exhibits less membranous basal-layer β-catenin expression (green) with infrequent nuclear expression (for quantitation and immunohistochemical analysis, see Supplementary Figures S2 and S3, available at *Carcinogenesis* Online). (**F**) p-GSK3β expression in (upper) 4HT-treated versus (lower) untreated *K14.creP/lslROCK*^{er} ear skin shows stronger expression in 4HT-treated epidermis becoming stronger and more uniform with time in (**G**) older (12 weeks) 4HT/RU486-treated *K14.creP/lslROCK*^{er} hyperplasia. Higher magnification (**H**) shows 4HT/RU486-treated *K14.creP/lslROCK*^{er} hyperplasia maintains elevated p-GSK3β expression in both basal and suprabasal layers; whereas (**I**) *HK1.ras* hyperplasia displays less p-GSK3β that weakens in basal layers by 8 weeks and becomes increasingly supra-basal; again in parallel to β-catenin (for quantitation, see Supplementary Figure S4, available at *Carcinogenesis* Online). (**J** and **K**) p-AKT1 analysis in 4HT/RU486-treated *K14.creP/lslROCK*^{er} epidermis (4 weeks) shows elevated basal-layer expression compared with (**L**) sporadic, supra-basal p-AKT expression in normal adult skin; yet similar to (**M**) normal neonatal skin (24 h) that exhibits uniform, supra-basal p-AKT1. (**N**) Older (12 weeks) 4HT/RU486-treated *K14.creP/lslROCK*^{er} epidermis retains elevated p-AKT1, but with areas of supra-basal expression; similar to neonates. (**O**) *HK1.ras* hyperplasia (4–5 weeks) displays supra-basal and increasingly sporadic areas of p-AKT1 (for quantitation, see Supplementary Figure S5, available at *Carcinogenesis* Online). Bars: G, H and J ~120 μm; A, C, P and N ~80 μm; B, E, I, O and Q ~50 μm; Q, D, L and M ~30 μm).

with *HK1.ras* activation was unclear. Previously ROCK^{er} cooperation with *HK1.ras* activation-induced malignant conversion via p53 loss in papillomas and p21 loss following malignant conversion; where inhibition of early-stage malignant progression was also associated with a p21 antagonism to p-AKT1- and ROCK^{er}-associated NF-κB expression (18). Therefore, p53,

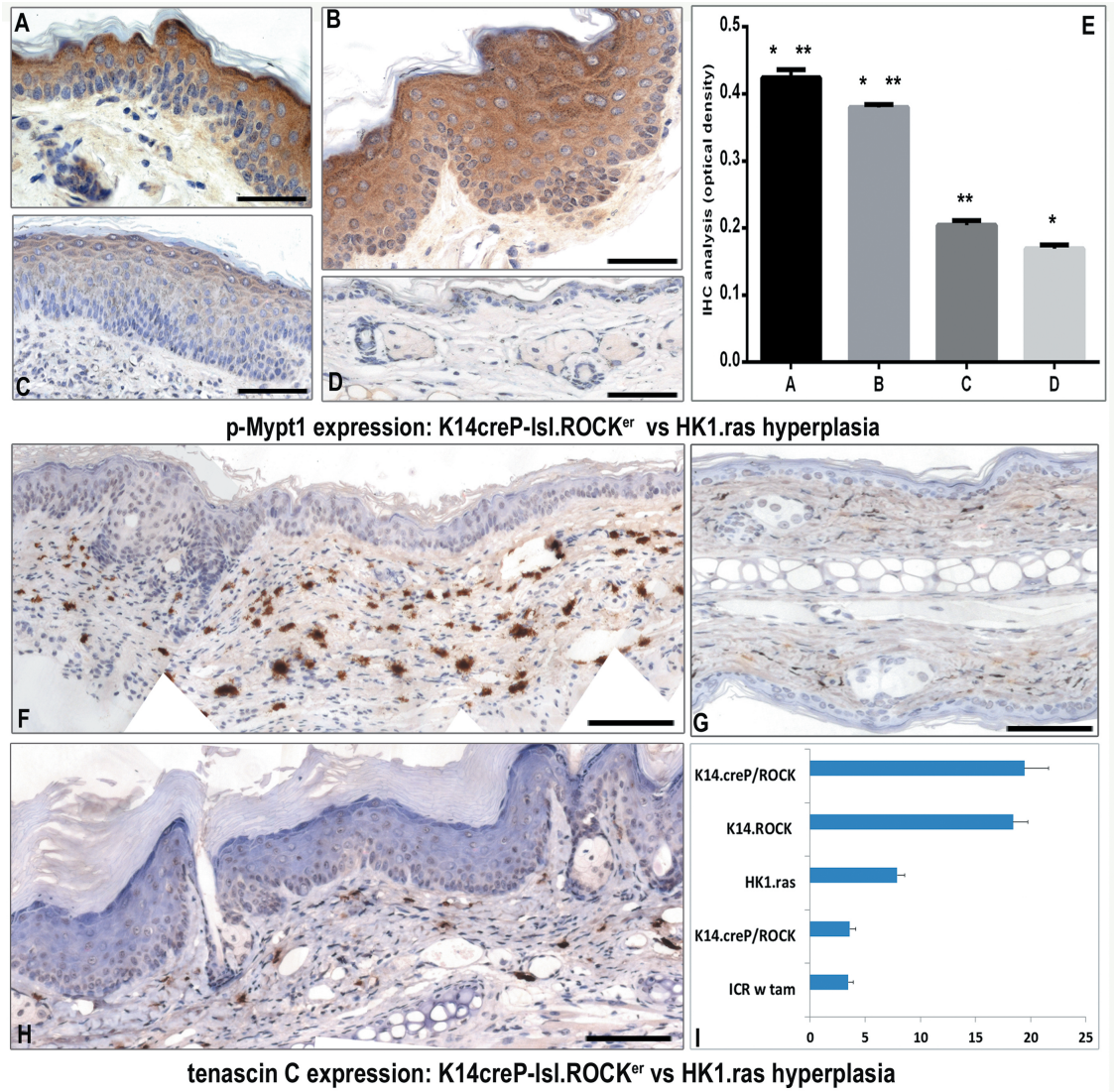

Figure 5. Analysis of p-Mypt1 and tenascin C expression in *K14.creP/lslROCK*^{er}. (**A**) 4HT/RU486-treated *K14.creP/lslROCK*^{er} epidermis at (12 weeks) shows ROCK^{er}-activated p-Mypt1 expression in all layers is (**B**) maintained over time (24 weeks) compared with (**C**) equivalent 4HT/RU486-treated *HK1.ras* hyperplasia (**$P < 0.001$; A and B versus C) or (**D**) control RU486-treated *K14.creP/lslROCK*^{er} epidermis (*$P < 0.001$; A and B versus D). (**F**) 4HT/RU486-treated *K14.creP/lslROCK*^{er} skin shows little epidermal tenascin C expression but numerous tenascin C^{+ve} cells appear in reticular/papillary dermis, with a halo of diffuse ECM expression. (**G**) RU486-alone treated *K14.creP/lslROCK*^{er} dermis exhibits sporadic tenascin C^{+ve} cells, while (**H**) *HK1.ras* dermis exhibits fewer tenascin C^{+ve} cells that lack diffuse, ECM expression. (**I**) Quantitation of dermal tenascin C^{+ve} cells (per 250 μm skin; averaged from 30 micrographs): 4HT/RU486-treated *K14.creP/lslROCK*^{er} (19.43 ± 2.21); *K14.ROCK*^{er} (18.40 ± 1.43); *HK1.ras*-induced hyperplasia (7.09 ± 1.43); RU486-alone treated *K14.creP/lslROCK*^{er} (3.6 ± 0.55); non-transgenic control skin (3.45 ± 0.47). Bars: F ~160 μm; H ~140 μm; E ~100 μm; A and B ~75 μm; C, D and G ~50 μm.

p21 and NF-κB status were assessed in *K14.creP/lslROCK*^{er} hyperplasia and contrasted to *HK1.ras* mice (Figure 6).

Hyperplastic, RU486-4HT-treated *K14.creP/lslROCK*^{er} shows elevated p53 expression appeared in both basal and supra-basal layers by 5–6 weeks (Figure 6A and B); whereas equivalent *HK1.ras* hyperplasia displays only sporadic p53 (Figure 6C) (**$P < 0.001$; A and B versus C), as elevated p53 appears in overt papillomas to inhibit conversion (24). Untreated *K14.creP/lslROCK*^{er} epidermis also displays sporadic p53 as specific keratinocytes complete the cell cycle (Figure 6D) (*$P < 0.001$; A and B versus D). Similarly serial sections from RU486/4HT-treated *K14.creP/lslROCK*^{er} demonstrated high p21 expression in all layers (Figure 6E and F); unlike *HK1.ras* hyperplasia which lacks p21 again until overt papillomas form (Figure 6G) (**$P < 0.001$; E and F versus G). Untreated, normal *K14.creP/lslROCK*^{er} epidermis possessed occasional weak, basal and supra-basal p21 expression as cells commit to differentiation (Figure 6H) (*$P < 0.001$; E and F versus H). Keratinocyte proliferation rates were assessed (Supplementary Figure S1, available at *Carcinogenesis* Online) and expressed as BrdU-labelled cells per mm of basement membrane. Consistent with p53/p21 observations, 4HT-treated *K14.creP/lslROCK*^{er} hyperplasia gave a mitotic index (12.1 ± 2.6) approximately double that of normal epidermis (3.7 ± 1.2) but less than *HK1.ras* epidermis (20.2 ± 6.1); hence a milder hyperplasia.

Analysis of NF-κB in treated *K14.creP/lslROCK*^{er} compared with *HK1.ras* hyperplasia (Figure 6I–L) shows the beginnings of increased NF-κB expression in all layers compared with untreated *K14.creP/lslROCK*^{er} ep (Figure 6I–K) (*$P < 0.05$; I and J versus K) or RU486/4HT-treated *HK1.ras* hyperplasia (Figure 6L (**$P < 0.05$; I and J versus L) which was similar to normal epidermis. Thus,

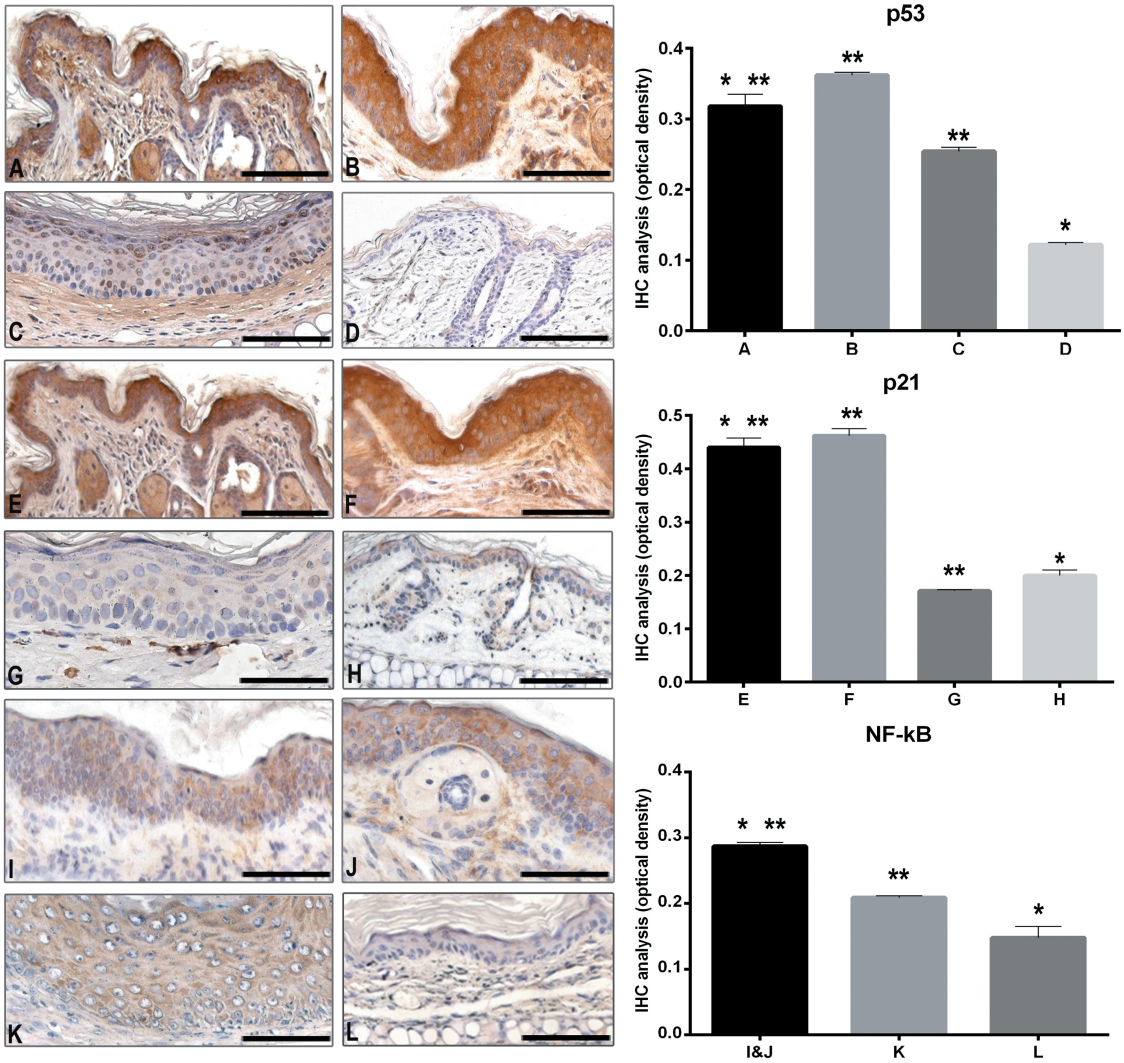

Figure 6. Analysis of p53, p21 and NF-κB expression in *K14.creP/lslROCK*^{er} and *HK1.ras* hyperplasia. (**A**) 4HT/RU486-treated *K14.creP/lslROCK*^{er} epidermis (6 weeks) shows elevated p53 expression in basal layer keratinocyte cytoplasm/nuclei, becoming (**B**) expressed in all layers (12 weeks). In comparison (**C**) *HK1.ras* hyperplasia (6 weeks) displays weak p53 in sporadic keratinocytes (**P < 0.001; A and B versus C); while (**D**) untreated *K14.creP/lslROCK*^{er} epidermis displays little detectable p53 (**P < 0.001; A and B versus D). (**E** and **F**) 4HT/RU486-treated *K14.creP/lslROCK*^{er} epidermis (6 weeks) exhibits elevated basal-layer p21 in nuclei and cytoplasm, becoming uniform in all layers by 12 weeks. (**G**) *HK1.ras* hyperplasia (6 weeks) exhibits occasional, supra-basal p21 expression (**P < 0.001; E and F versus G); similar to (**H**) RU486 alone-treated *K14.creP/lslROCK*^{er} epidermis (*P < 0.001; E and F versus H). (**I** and **J**) 4HT/RU486-treated epidermis shows low yet detectable NF-κB expression (12 weeks) in basal-layer keratinocytes compared with (**K**) 4HT/RU486-treated *HK1.ras* hyperplasia (**P < 0.05; I and J versus K) or (**L**) normal RU486-treated *K14.creP/lslROCK*^{er} epidermis that express little detectable NF-κB (*P < 0.05; I and J versus L). Bars: D and H ~90–100 μm; A and E 80–90 μm; B, C, K and L ~70–75 μm; I and J ~50–60 μm; G ~30 μm.

in this pre-neoplastic context, p21/p53 responses coupled to increased/premature differentiation counter effects of AKT1/β-catenin signalling and/or ROCK^{er}-associated NF-κB expression, to help inhibit ROCK^{er}-mediated papillomatogenesis.

Discussion

Inducible, ROCK2-mediated deregulation of the actinomyosin cytoskeleton in cutaneous keratinocytes resulted in epidermal hyperplasia with an altered differentiation profile, together with changes in dermal fibroblasts indicative of an altered ECM. Hyperplasia resulting from increased keratinocyte proliferation is consistent with *ROCK/Rho* family members being downstream effectors of ras signalling (3), and activation of AKT/GSK3β/β-catenin axis; which also contributed to a rigid skin (6). Here, ROCK^{er}/β-catenin-associated increases in dermal collagen deposition establishes a mechano-transduction feedback loop via FAK/AKT-mediated, α6/β4 integrin signalling, that maintains hyperplasia and rigidity to lay down foundations for subsequent carcinogenesis (6,9–15,27,28). However in this pre-neoplastic context, unlike *HK1.ras* activation, responses to ROCK^{er}-activated basal layer p-AKT1 and nuclear/membranous β-catenin immediately induced p53/p21 expression that limited keratinocyte proliferation and accelerated differentiation that, together with minimized NFκB expression, inhibited papillomatogenesis.

These ROCK^{er}-specific, premature/accelerated differentiation responses, echo (and may subvert) normal ROCK2 roles in epidermal homeostasis. In sync with appropriate IF expression, these roles are essential for embryonic epidermal barrier formation and to maintain tensile strength of differentiated epidermal layers in adult skin (7,8). Thus, normal epidermis shows ROCK2 expression in differentiated, supra-basal layers increases following induction of keratinocyte differentiation *in vitro*, together with targets p-MLC/p-Myp (Figures 1, 2 and

5) (5,9) consistent with a co-ordinated response between the IF and actinomyosin cytoskeleton networks as keratinocytes commit to differentiate (7,8). Hence, anomalous ROCK^{er} activation and p-MLC/p-MypT expression in proliferative basal keratinocytes gave a resultant hyperplasia exhibiting an altered differentiation milieu (keratin K1, loricrin and filaggrin); while changes in epidermal flexibility/keratinocyte motility may alter expression of hyperproliferative/stress keratins, for example, K6α, that likely reflect roles in wounding (below). As *K14.creP/lslROCK^{er}* mice exhibited anomalous K1 in keratinocytes cultured in low Ca^{2+} and premature increased keratin K1 expression *in vivo*, with a ragged appearance to the K1/K14 border; it suggests basal-layer ROCK^{er} activation induced a premature commitment to differentiate, an idea also supported by increased/premature filaggrin and loricrin expression (Figure 3). The confused nature of the differentiation marker milieu may centre on anomalous ROCK^{er}-activated p-AKT1 activation in basal layer keratinocytes (below); alongside β-catenin-mediated alteration of, for example, integrin signalling and focal adhesion turnover (6,9,11,29). Alternate signalling in *HK1.ras* hyperplasia support this idea, given the ordered nature of the K1/K14 border as keratinocytes committed to differentiate, and that reduced filaggrin/loricrin was paralleled by diminishing and increasingly suprabasal p-AKT1/β-catenin expression (Figure 4).

Furthermore in *K14.creP/lslROCK^{er}* epidermis, accelerated/premature expression of IF molecules that contribute to ROCK^{er}/p-Mypt1-mediated changes in epidermal rigidity (6), may in turn inhibit papilloma formation. Previously, increased differentiation responses enforced by expression of K1 (or K10) inhibited ras-driven carcinogenesis (30,31). Moreover, cessation of 4HT-treatment in *HK1.ras/K14.ROCK^{er}* carcinogenesis that demonstrated loss of *ROCK^{er}* expression reduced tumour size also proceeded via a mechanism of increased K1-associated, differentiation (18). Moreover, it may be that premature K1 expression reflects epidermal responses to *ROCK^{er}*-mediated p-AKT activation in basal layer keratinocytes. In normal adult epidermis, interfollicular p-AKT1 expression was sporadic and suprabasal, whereas in neonatal epidermis p-AKT1 expression is uniform and co-localized with supra-basal K1 (Figure 4). This feature maybe geared to counter potential threats to early barrier maintenance from, for example, p53-mediated apoptosis while p53 completes DNA scrutiny in the naturally hyperproliferative basal-layer keratinocytes; and thus AKT1 gives time for keratinocytes to commit to terminal differentiation not apoptosis (24,32). Hence, ROCK^{er}-mediated basal-layer p-AKT1 in adults signalled a premature commitment to differentiation manifest by increased, ragged K1 expression that helps inhibit papillomatogenesis; whereas *HK1.ras* hyperplasia exhibits sporadic, supra-basal p-AKT1; and K1 expression is delayed, yet ordered.

Another aspect of epidermal differentiation unique to *K14.creP/lslROCK^{er}* hyperplasia, was the lack of keratin K6α expression, a hair follicle marker associated with hyperproliferative, stressed or wound conditions (8,33,34). Treated *K14.creP/lslROCK^{er}* epidermis exhibited reduced/patchy K6α expression, often localized to troughs of papillomatous (folded/convoluted) hyperplasia, compared with the uniform strong expression typified by *HK1.ras* hyperplasia before papilloma formation. *In vitro*, strong K6α expression observed in normal, proliferative keratinocytes, was virtually absent in RU486/4HT-treated *K14.creP/lslROCK^{er}* keratinocytes (Figure 3). These observations may reflect ROCK2 roles in epidermal rigidity/flexibility and those that regulate motility/flexibility at the cellular level following wounding. Both ROCK1 and ROCK2 are necessary for migratory responses in wounding, consistent with the finding that epidermal ROCK^{er} expression accelerates healing of cutaneous full thickness wounds (2,4,35). Thus, ROCK^{er}-activated/p-MLC/p-Mypt1-regulated changes coupled to premature expression of K1/loricrin/filaggrin (above) that increase epidermal rigidity, may combine to reduce K6α in attempts to maintain tissue flexibility. If correct, this idea partly explains the localization of K6α expression in troughs of folded/papillomatous hyperplasia and is an idea supported by full-thickness wounding of K6α/β knockout mice that also display increased K1/K10 co-expression to increase tissue rigidity to counter cell fragility in a wounded skin (33,34).

Further, at the cellular level reduced K6α expression [and partner keratin K16 (36)] may represent an intermediate state of rigidity/flexibility geared to help initiate keratinocyte proliferation early in wound healing (33). This would facilitate subsequent ROCK-associated keratinocyte migration (2,34,36); as suggested by analysis of cell migration observed at wound margins in K6α/β knockout mice that demonstrates F-actin expression at the leading edge (34), indicative of the localized ROCK1/2 roles in cell motility (2–4). These data highlight the balance between stress/wound-associated K6α/β/K16 (35,36) IFs and the ROCK-associated actinomyosin cytoskeleton in the cellular/tissue flexibility/motility necessary to maintain migration versus rigidity for epidermal homeostasis in wounding (2); where deregulation of this balance may facilitate the increased motility/rigidity observed in skin cancer (6,12,15,18).

Indeed, as evidenced from *in vitro* interfollicular stem cell lineage studies (37), it may be that ROCK2 has a pivotal role in regulating the balance between proliferation and differentiation to maintain epidermal homeostasis, as suggested in the wound response (above). This *in vitro* study (and reports referenced therein), shows that ROCK signalling is essential to stem cell population decisions to proliferate and maintain either a confluent, quiescent colony or an expanding one. In this model, as human stem cell keratinocytes cultured on feeder layers establish colonies that approach local confluence, ROCK2 kinase activities were instrumental in the decision to switch from an expansion phase, where proliferation dominates over differentiation, to one of balance where keratinocyte proliferation replaces only those cells committed to differentiation (37). Furthermore, in scratch assays that mimic wounding, ROCK2 signalling was also essential to reverse this decision and change from the balanced mode and return to the expanding phase (37). These data would be consistent with roles observed in cell migration (2,4,33–36) and with the findings in this transgenic skin model regarding anomalous, inducible basal layer ROCK^{er} expression that clearly disturbs the respective balanced versus expansion proliferation modes. That this leads to an overall hyperplasia which also exhibits premature differentiation marker expression, further reflects the importance of ROCK2 signalling in the commitment to proliferate (37), differentiate (5) and the responses geared to enhanced wounding/cell migration (2) or threats to maintenance of the paramount barrier function (12).

Thus, a surprising finding in this ROCK^{er} model was the lack of spontaneous papillomatogenesis and this highlights the ability of tissues to inhibit early-stage carcinogenesis, particularly in skin evolved to constantly cope with environmental carcinogens. The data outlined above suggest an epidermis employs differentiation-specific responses to ROCK^{er}-mediated p-AKT1/GSK3β/β-catenin deregulation to inhibit papilloma. In addition, this axis appears to induced an immediate, elevated p53/p21 expression; a response absent in *HK1.ras* hyperplasia destined to produce papillomas. In this instance, anomalous

ROCK^{er}-mediated β-catenin/Wnt signalling may be a major facet that induced p53, as previously β-catenin knockout blocked ROCK^{er} phenotypes (6). Such compensatory p53 expression was observed previously in this model, alongside p-AKT-induced p21 expression (18,24); while in colon carcinogenesis APC^{null}-mediated nuclear β-catenin induced transcriptionally active p53 (38–40). Further, ROCK signalling in focal adhesion turnover (9) shows FAK expression supresses Rho activity and ROCK2 compensates for FAK loss (10). Thus, it is noteworthy that FAK deletion also demonstrates p53-mediated induction of p21 (41) as observed for ROCK (19); that also links to β-catenin, as FAK overexpression is a necessary downstream event of APC/β-catenin/WNT signalling (29,42), which presumably circumvents compensatory p53/p21 inhibition (24,29,39–42).

Here, p53/p21 expression in *K14.creP/lslROCK*^{er} hyperplasia successfully counters threats from membranous/nuclear β-catenin/p-AKT1 expression via a reduced proliferation rate; elevated p53-mediated protection against additional mutations and increased p21-associated differentiation responses (42); yet avoids excessive p53/p21 induced apoptosis due to continued p-AKT1/p53 antagonism that maintains the paramount barrier function (above) (25,32). Indeed older 4HT/RU486-treated *K14.creP/lslROCK*^{er} epidermis retained the elevated, interfollicular p-AKT1 observed in neonates, suggesting ROCK^{er} established a more juvenile epidermal context that initially paralleled β-catenin/p-GSK3β expression (27). However, with time, p-AKT1 expression became increasingly supra-basal; possibly as a consequence of p21 expression; now inhibiting the potential for p-AKT1-associated papillomatogenesis. Accordingly, *HK1.ras* hyperplasia displayed a sporadic, supra-basal p-AKT1 expression profile paralleled by increasingly supra-basal β-catenin expression; suggesting that in ras-driven papillomatogenesis AKT1 appears causal at later stages (Greenhalgh *et al.*, in preparation).

Another major pathway previously implicated in *HK1.ras/K14.ROCK*^{er} carcinogenesis involved canonical *NF-κB* signalling (20,43–46) and linked ROCK^{er}-associated NF-κB expression with the latter stages of malignant conversion and progression (18,20). *NF-κB* signalling has a long association with effecting inflammatory responses; yet transcriptional roles also regulate proliferation, apoptosis and cell migration (43). In *K14.creP/lslROCK*^{er} hyperplasia, initial cross-talk between *ROCK*^{er} and *NF-κB* signalling would contribute to increased proliferation (18); but increasing p21 (18,19) and p53 (18,44) apparently reduced NF-κB expression to weak, yet detectable levels. In this instance, p21 rather than p53 maybe the significant facet of ROCK^{er}-specific NF-κB inhibition (19,45), as previously *HK1.ras/K14.ROCK*^{er} carcinogenesis identified a distinct antagonism between p21 and NF-κB; as regressing tumours following 4HT-cessation displayed intense, basal-layer p21 which restricted/returned NF-κB (and p-AKT1) to the supra-basal expression profile observed in papillomas (18). A result also consistent with liver carcinogenesis, where NEMO, a major NF-kB regulator, requires p21 loss for NEMO-driven tumour progression (45,46); and *HK1.ras/K14.ROCK*^{er} carcinogenesis where p21 loss allows ROCK^{er}-mediated NF-κB to combine with unregulated p-AKT1 to achieve malignancy. These data strengthen links between ROCK^{er}/NF-κB and also indirectly link NF-κβ signalling to stromal remodelling that predisposes to tumour progression via expression of ECM molecules, such as tenascin C (47).

An altered stromal ECM is an essential factor for carcinogenesis, aiding tumour cell survival and providing the permissive environment for cellular invasion and tenascin C is one of the most relevant molecules mediating changes to the dermal ECM, reflecting both tumour aggression and metastatic potential (28). Tenascin C overexpression is already associated with activated Rho/Rock and MAP Kinase signalling (15,18), with links to NF-κβ roles in inflammation and deregulated apoptosis (47), that may protect initiating cancer stem cells leading to tumour relapse (48). Thus, in *K14.creP/lslROCK*^{er} mice altered mechano-signalling via epidermal MLC/Mypt1 phosphorylation; coupled to ROCK^{er}/β-catenin-associated deposition of collagen/fibrin, increases dermal ECM rigidity and one consequence apparently manifests as intense tenascin C expression in a specific sub-population of dermal fibroblasts.

Moreover, these tenascin C^{+ve} cells maybe precursors of cancer-associated fibroblasts (CAFs) (13), a sub-population of stromal cells that aid the invasion process by aligning collagen fibres to provide highways within the ECM for invading SCC cells (13,28,49). Indeed a predisposed, promoting role for such (pre-CAF) dermal cells is supported by the observation that in RDEB patients susceptible to SCC following injury (12), a population of wound-associated myofibroblasts alters the rigidity of the dermal microenvironment via a mechanism of increased integrin/FAK/AKT signalling similar to that observed in ROCK^{er} mice (6,12).

CAFs share many similarities with such myofibroblasts and are thought to arise from healthy dermal cells subverted by the new microenvironment conditions (13,28,49), such as those laid down in a ROCK^{er} dermis. Further, CAFs form anomalous adhesion junctions with invading SCC cells that triggers β-catenin recruitment and vinculin/α-catenin-dependent adhesion, establishing a feedback loop to increase rigidity of the tumour microenvironment that aids invasion (50). However, the mechanism by which normal fibroblasts evolve into CAFS is unclear; mainly due to the heterogeneity within the tumour microenvironment (13,28,49). Thus, it is noteworthy that anomalous, epidermal-specific β-catenin expression effects specific populations of dermal fibroblasts (14) and this suggests ROCK^{er}-mediated β-catenin expression may begin their evolution into a pre-CAF phenotype. Nonetheless, while fully evolved CAFs are essential for tissue invasion, providing an invasive highway from re-aligned collagen fibres and helping to maintain cancer stem cells (48,51) such tenascin^{+ve} (pre-CAF?) dermal fibroblasts appear unable to influence papillomatogenesis, in the absence of tumour promotion (6,12).

Collectively these data show that the cellular potential to achieve even a benign tumour depends upon specific genetic mutations pitted against inherent abilities within the cell/tissue microenvironment that resist the modified oncogenic circuitry. In *K14.creP/lslROCK*^{er} epidermis, papillomatogenesis awaits permissive events such as a constitutive promotion role currently under investigation; whereas a potent initiator such as *HK1.ras* expression or chemically induced ras^{Ha} activation achieves papilloma and circumvents these p53/p21 responses creating a context where ROCK^{er} drives tumour progression and invasion.

Supplementary material

Supplementary data are available at *Carcinogenesis* online.

Funding

This work was supported by the Government of Malaysia; the Scott Endowment Fund, Dermatology, Glasgow University; and Cancer Research UK.

Acknowledgements

We would like to thank Dr Jean Quinn for help and advice; Stuart Lannigan and Denis Duggan for assistance with animal husbandry.

Conflict of Interest Statement: None declared.

References

1. Olson, M.F. (2018) Rho GTPases, their post-translational modifications, disease-associated mutations and pharmacological inhibitors. *Small GTPases*, 9, 203–215.
2. Kular, J. *et al.* (2015) A negative regulatory mechanism involving 14-3-3ζ limits signaling downstream of ROCK to regulate tissue stiffness in epidermal homeostasis. *Dev. Cell*, 35, 759–774.
3. Kümper, S. *et al.* (2016) Rho-associated kinase (ROCK) function is essential for cell cycle progression, senescence and tumorigenesis. *Elife*, 5, e12994.
4. Julian, L. *et al.* (2014) Rho-associated coiled-coil containing kinases (ROCK): structure, regulation, and functions. *Small GTPases*, 5, e29846.
5. Lock, F.E. *et al.* (2009) Distinct roles for ROCK1 and ROCK2 in the regulation of keratinocyte differentiation. *PLoS One*, 4, e8190.
6. Samuel, M.S. *et al.* (2011) Actomyosin-mediated cellular tension drives increased tissue stiffness and β-catenin activation to induce epidermal hyperplasia and tumor growth. *Cancer Cell*, 19, 776–791.
7. Vaezi, A. *et al.* (2002) Actin cable dynamics and Rho/Rock orchestrate a polarized cytoskeletal architecture in the early steps of assembling a stratified epithelium. *Dev. Cell*, 3, 367–381.
8. Simpson, C.L. *et al.* (2011) Deconstructing the skin: cytoarchitectural determinants of epidermal morphogenesis. *Nat. Rev. Mol. Cell Biol.*, 12, 565–580.
9. Lock, F.E. *et al.* (2012) Differential regulation of adhesion complex turnover by ROCK1 and ROCK2. *PLoS One*, 7, e31423.
10. Seong, J. *et al.* (2013) Distinct biophysical mechanisms of focal adhesion kinase mechanoactivation by different extracellular matrix proteins. *Proc. Natl. Acad. Sci. USA*, 110, 19372–19377.
11. Irianto, J. *et al.* (2016) SnapShot: mechanosensing matrix. *Cell*, 165, 1820–1820.e1.
12. Mittapalli, V.R. *et al.* (2016) Injury-driven stiffening of the dermis expedites skin carcinoma progression. *Cancer Res.*, 76, 940–951.
13. Gascard, P. *et al.* (2016) Carcinoma-associated fibroblasts: orchestrating the composition of malignancy. *Genes Dev.*, 30, 1002–1019.
14. Lichtenberger, B.M. *et al.* (2016) Epidermal β-catenin activation remodels the dermis via paracrine signalling to distinct fibroblast lineages. *Nat. Commun.*, 7, 10537.
15. Sarassa-Renedo, A. *et al.* (2006) Role of RhoA/ROCK-dependent actin contractility in the induction of tenascin-C by cyclic tensile strain. *Exp. Cell Res.*, 312, 1361–1370.
16. Rath, N. *et al.* (2012) Rho-associated kinases in tumorigenesis: re-considering ROCK inhibition for cancer therapy. *EMBO Rep.*, 13, 900–908.
17. Unbekandt, M. *et al.* (2018) Discovery of potent and selective MRCK inhibitors with therapeutic effect on skin cancer. *Cancer Res.*, 78, 2096–2114.
18. Masre, S.F. *et al.* (2017) ROCK2/rasHa co-operation induces malignant conversion via p53 loss, elevated NF-κB and tenascin C-associated rigidity, but p21 inhibits ROCK2/NF-κB-mediated progression. *Oncogene*, 36, 2529–2542.
19. Olson, M.F. *et al.* (1998) Signals from ras and rho GTPases interact to regulate expression of p21Waf1/Cip1. *Nature*, 394, 295–299.
20. Benitah, S.A. *et al.* (2003) ROCK and nuclear factor-kappaB-dependent activation of cyclooxygenase-2 by Rho GTPases: effects on tumor growth and therapeutic consequences. *Mol. Biol. Cell*, 14, 3041–3054.
21. Greenhalgh, D.A. *et al.* (1993) Induction of epidermal hyperplasia, hyperkeratosis, and papillomas in transgenic mice by a targeted v-Ha-ras oncogene. *Mol. Carcinog.*, 7, 99–110.
22. Samuel, M.S. *et al.* (2016) Tissue-selective expression of a conditionally-active ROCK2-estrogen receptor fusion protein. *Genesis*, 54, 636–646.
23. Berton, T.R. *et al.* (2000) Characterization of an inducible, epidermal-specific knockout system: differential expression of lacZ in different Cre reporter mouse strains. *Genesis*, 26, 160–161.
24. Macdonald, F.H. *et al.* (2014) PTEN ablation in Ras(Ha)/Fos skin carcinogenesis invokes p53-dependent p21 to delay conversion while p53-independent p21 limits progression via cyclin D1/E2 inhibition. *Oncogene*, 33, 4132–4143.
25. Croft, D.R. *et al.* (2006) Conditional regulation of a ROCK-estrogen receptor fusion protein. *Methods Enzymol.*, 406, 541–553.
26. Greenhalgh, D.A. *et al.* (1989) Spontaneous rasHa activation in cultured primary murine keratinocytes: consequences of rasHa activation in malignant conversion and malignant progression. *Mol. Carcinog.*, 3, 154–161.
27. Collins, C.A. *et al.* (2011) Reprogramming adult dermis to a neonatal state through epidermal activation of β-catenin. *Development*, 138, 5189–5199.
28. Lowy, C.M. *et al.* (2015) Tenascin C in metastasis: a view from the invasive front. *Cell Adh. Migr.*, 9, 112–124.
29. Ashton, G.H. *et al.* (2010) Focal adhesion kinase is required for intestinal regeneration and tumorigenesis downstream of Wnt/c-Myc signaling. *Dev. Cell*, 19, 259–269.
30. Kartasova, T. *et al.* (1992) Relationship between the expression of differentiation-specific keratins 1 and 10 and cell proliferation in epidermal tumors. *Mol. Carcinog.*, 6, 18–25.
31. Santos, M. *et al.* (2002) The expression of keratin k10 in the basal layer of the epidermis inhibits cell proliferation and prevents skin tumorigenesis. *J. Biol. Chem.*, 277, 19122–19130.
32. Calautti, E. *et al.* (2005) Phosphoinositide 3-kinase signaling to Akt promotes keratinocyte differentiation versus death. *J. Biol. Chem.*, 280, 32856–32865.
33. Wojcik, S.M. *et al.* (2000) Delayed wound healing in keratin 6a knockout mice. *Mol. Cell. Biol.*, 20, 5248–5255.
34. Wong, P. *et al.* (2003) Loss of keratin 6 (K6) proteins reveals a function for intermediate filaments during wound repair. *J. Cell Biol.*, 163, 327–337.
35. Chen, B.H. *et al.* (2002) Roles of Rho-associated kinase and myosin light chain kinase in morphological and migratory defects of focal adhesion kinase-null cells. *J. Biol. Chem.*, 277, 33857–33863.
36. Maruthappu, T. *et al.* (2017) Rhomboid family member 2 regulates cytoskeletal stress-associated Keratin 16. *Nat. Commun.*, 8, 14174.
37. Roshan, A. *et al.* (2016) Human keratinocytes have two interconvertible modes of proliferation. *Nat. Cell Biol.*, 18, 145–156.
38. Clevers, H. *et al.* (2012) Wnt/β-catenin signaling and disease. *Cell*, 149, 1192–1205.
39. Damalas, A. *et al.* (2001) Deregulated beta-catenin induces a p53- and ARF-dependent growth arrest and cooperates with Ras in transformation. *EMBO J.*, 20, 4912–4922.
40. Ghosh, J.C. *et al.* (2005) Activation of p53-dependent apoptosis by acute ablation of glycogen synthase kinase-3beta in colorectal cancer cells. *Clin. Cancer Res.*, 11, 4580–4588.
41. Graham, K. *et al.* (2011) FAK deletion promotes p53-mediated induction of p21, DNA-damage responses and radio-resistance in advanced squamous cancer cells. *PLoS One*, 6, e27806.
42. Topley, G.I. *et al.* (1999) p21(WAF1/Cip1) functions as a suppressor of malignant skin tumor formation and a determinant of keratinocyte stem-cell potential. *Proc. Natl. Acad. Sci. USA*, 96, 9089–9094.
43. Karin, M. (2006) NF-kappaB and cancer: mechanisms and targets. *Mol. Carcinog.*, 45, 355–361.
44. Webster, G.A. *et al.* (1999) Transcriptional cross talk between NF-kappaB and p53. *Mol. Cell. Biol.*, 19, 3485–3495.
45. Ehedego, H. *et al.* (2015) p21 ablation in liver enhances DNA damage, cholestasis, and carcinogenesis. *Cancer Res.*, 75, 1144–1155.
46. Ma, W. *et al.* (2016) RhoE/ROCK2 regulates chemoresistance through NF-κB/IL-6/ STAT3 signaling in hepatocellular carcinoma. *Oncotarget*, 7, 41445–41459.
47. Shi, M. *et al.* (2015) Tenascin-C induces resistance to apoptosis in pancreatic cancer cell through activation of ERK/NF-κB pathway. *Apoptosis*, 20, 843–857.
48. Jachetti, E. *et al.* (2015) Tenascin-C protects cancer stem-like cells from immune surveillance by arresting T-cell activation. *Cancer Res.*, 75, 2095–2108.
49. Kalluri, R. (2016) The biology and function of fibroblasts in cancer. *Nat. Rev. Cancer*, 16, 582–598.
50. Labernadie, A. *et al.* (2017) A mechanically active heterotypic E-cadherin/N-cadherin adhesion enables fibroblasts to drive cancer cell invasion. *Nat. Cell Biol.*, 19, 224–237.
51. Su, S. *et al.* (2018) $CD10^{+}GPR77^{+}$ Cancer-associated fibroblasts promote cancer formation and chemoresistance by sustaining cancer stemness. *Cell*, 172, 841.e16–856.e16.